Targeted genetic analysis of cerebral blood flow imaging phenotypes implicates the *INPP5D* gene

Xiaohui Yao[a], Shannon L. Risacher[b], Kwangsik Nho[b], Andrew J. Saykin[b], Ze Wang[c,*], Li Shen[a,*], for the Alzheimer's Disease Neuroimaging Initiative[1]

[a] Department of Biostatistics, Epidemiology and Informatics, Perelman School of Medicine, University of Pennsylvania, Philadelphia, PA 19104, USA

[b] Department of Radiology and Imaging Sciences, Indiana University School of Medicine, Indianapolis, IN 46202, USA

[c] Department of Diagnostic Radiology and Nuclear Medicine, University of Maryland School of Medicine, Baltimore, MD 21201, USA

[1] Data used in preparation of this article were obtained from the Alzheimer's Disease Neuroimaging Initiative (ADNI) database (adni.loni.usc.edu). As such, the investigators within the ADNI contributed to the design and implementation of ADNI and/or provided data but did not participate in analysis or writing of this report. A complete listing of ADNI investigators can be found at: http://adni.loni.usc.edu/wp-content/uploads/how_to_apply/ADNI_Acknowledgement_List.pdf

[*] **Correspondence to:**

Li Shen, B306 Richards Building, 3700 Hamilton Walk, Philadelphia, PA 19104, USA;
E-mail: Li.Shen@pennmedicine.upenn.edu

Ze Wang, 670 W Baltimore Ave, Room 1173, Baltimore MD 21201, USA;
E-mail: ze.wang@som.umaryland.edu

Abstract

The vascular hypothesis of Alzheimer's disease (VHAD) has proposed the involvement of brain hypoperfusion in AD pathogenesis, where cognitive decline and dysfunction result from dwindling cerebral blood flow (CBF). Based on the VHAD, we focused on exploring how genetic factors influence AD pathogenesis via the cerebrovascular system. To investigate the role of CBF endophenotypes in AD pathogenesis, we performed a targeted genetic analysis of 258 subjects from the ADNI cohort to examine associations between 4,033 SNPs of 24 AD genes and CBF measures in four brain regions. A novel association with CBF measure in the left angular gyrus (L-AG) was identified in an *INPP5D* SNP (i.e., rs61068452; *P* = 1.48E-7; corrected *P* = 2.39E-3). The gene-based analysis discovered both *INPP5D* and *CD2AP* associated with the L-AG CBF. Further analyses on non-overlapping samples revealed that rs61068452-G was associated with lower CSF t-tau/$A\beta_{1-42}$ ratio. Our findings suggest a protective role of rs61068452-G in an AD-relevant cerebrovascular endophenotype, which has the potential to provide novel insights for better mechanistic understanding of AD.

Keywords: Alzheimer's disease; cerebral blood flow; genetics; *INPP5D*; neurovascular

1. Introduction

Alzheimer's disease (AD) is a complex degenerative disease of the brain, characterized by neurodegeneration, memory impairment and cognitive problems (Jack *et al.*, 2010). As the leading cause of dementia, AD is influenced by environmental and genetic factors. It is critical to improve the understanding of molecular mechanisms of AD because of its high prevalence, burdens, and currently no cure. Genome-wide association studies (GWAS) of quantitative endophenotypes have successfully identified a number of loci susceptible for AD (Saykin *et al.*, 2015), however, the underlying molecular mechanisms of how these genetic factors modulate AD or its biomarkers are not well characterized.

The vascular hypothesis of Alzheimer's disease (VHAD) (de la Torre, 2018) has proposed the involvement of brain hypoperfusion in AD pathogenesis, where cognitive decline and dysfunction result from dwindling neuronal energy supply and oxidative stress. In support of the vascular hypothesis, evidence suggests measurement of cerebral blood flow (CBF) may be a promising indicator of brain hypoperfusion useful for early detection of AD and assessing disease progression (Zhang *et al.*, 2017). Consistent with the vascular hypothesis of AD, recent results have also demonstrated the potential of CBF as biomarker for preclinical detection of AD, as CBF changes present long before amyloid β (Aβ) load or brain atrophy (Hays *et al.*, 2016). Other studies have discovered the association of CBF with AD stages as well as various brain structural and functional imaging quantitative traits (Chen *et al.*, 2011; Musiek *et al.*, 2012; Wang *et al.*, 2013; Mattsson *et al.*, 2014; Michels *et al.*, 2016; Bangen *et al.*, 2017). However, the molecular mechanisms of CBF changes underlying AD have not been fully understood.

Given that large variations of CBF have been seen across AD studies, high scientific interests have aroused to examine whether they have a genetic basis. Reciprocally, assessing the genetic association with CBF might provide a better understanding of molecular mechanisms underlying changes of CBF as well as gaining additional insight into complex neurodegenerative diseases. To the best of our knowledge, the genetic contributions to CBF is an under-explored topic in AD research, except that a few studies examined the *APOE* effects on CBF (Kim *et al.*, 2013b; Hays *et al.*, 2016). Accordingly, in this study, we propose to investigate the genetic factors that affect AD through regulating the function of cerebrovascular system.

GWAS have successfully identified a number of loci susceptible for complex neurological traits and diseases (Saykin *et al.*, 2015). Recently, a large scale meta-analysis of GWAS identified a set of susceptibility loci for late-onset AD (LOAD), including 9 known and 12 new

single nucleotide polymorphisms (SNPs) (Lambert *et al.*, 2013). In addition to *APOE*, 23 genes underlying these 21 significant variants are discovered, most of which are associated with inflammation and immune system. For example, there are several genes encoding proteins relevant to microglial function and inflammation, including *TREM2*, *CD33*, *CR1*, *ABCA7* and *INPP5D* (Malik *et al.*, 2015). Mechanisms of how these genetic factors modulate AD or its biomarkers remain to be discovered.

Based on the VHAD, we hypothesized that some genetic factors impact AD pathogenesis via influencing brain hypoperfusion. Thus, this study is designed to improve the understanding of mechanisms by which genetic factors impact AD pathogenesis, in this case by investigating the role of cerebrovascular functions as an AD endophenotypes. Therefore, in this study, we perform a targeted genetic analysis for exploring the genetic effect on CBF measures in four brain regions using 24 AD candidate genes (*APOE* and the other 23 reported AD genes mentioned above), to help provide novel insights for better revealing molecular interpretation of AD. To evaluate the CBF genetic findings, we further examine non-overlapping samples from the Alzheimer's Disease Neuroimaging Initiative (ADNI) cohort regarding their associations with the CSF t-tau/$A\beta_{1\text{-}42}$ ratio and FDG-PET glucose metabolism, given that both are established AD biomarkers and their abnormalities have been suggested as downstream pathological events from initiation of brain hypoperfusion under VHAD (de la Torre, 2018). In addition, to examine whether our most significant CBF genetic finding has a direct effect on AD, we further evaluated its association with the AD status using the summary statistics from the most recent genome-wide meta-analysis of AD (Jansen *et al.*, 2019).

2. Materials and Methods

2.1. Alzheimer's Disease Neuroimaging Initiative

Data used in the preparation of this article were obtained from the ADNI database (adni.loni.usc.edu). The ADNI was launched in 2003 as a public-private partnership, led by Principal Investigator Michael W. Weiner, MD. The primary goal of ADNI has been to test whether serial MRI, PET, other biological markers, and clinical and neuropsychological assessment can be combined to measure the progression of mild cognitive impairment (MCI) and early AD. For up-to-date information, see www.adni-info.org.

2.2. Genome-wide meta-analysis of AD

A large genome-wide meta-analysis of clinically diagnosed AD and AD-by-proxy was recently conducted (Jansen et al., 2019). The study included three phases: (1) Phase 1 was a meta-

analysis of the AD status (*N* = 79,145) using three independent cohorts collected by Alzheimer's disease working group of the Psychiatric Genomics Consortium (PGC-ALZ), the International Genomics of Alzheimer's Project (IGAP), and the Alzheimer's Disease Sequencing Project (ADSP). (2) Phase 2 was a GWAS of the AD-by-proxy status (*N* = 376,113), using individuals of European ancestry from the UK Biobank with parental AD status weighted by age. (3) Phase 3 was a meta-analysis of the Phase 1 and Phase 2 findings, with totally 455,258 samples (71,880 cases and 383,378 controls). In this work, we downloaded the summary statistics of the Phase 3 analysis (available at https://ctg.cncr.nl/software/summary_statistics) to examine whether our CBF finding is associated with AD.

2.3. Study participants

Participants for the current CBF study were limited to those with baseline scans from ADNI in the ASL MRI sub study as of May 2012. Full inclusion and exclusion criteria for ADNI are described at www.adni-info.org. Detailed quality control (QC) steps for phenotypic and genotypic data had been previously reported (Kim *et al.*, 2013a; Wang *et al.*, 2013) and were briefly described below. Participants were restricted to non-Hispanic Caucasian to reduce the likelihood of population stratification effects in the genetic analysis. A total of 258 non-Hispanic Caucasian subjects whose CBF data met all QC criteria were analyzed, including 72 healthy control (HC), 16 significant memory concern (SMC), 71 early mild cognitive impairment (EMCI), 57 late mild cognitive impairment (LMCI) and 42 AD participants. Detailed characteristic information and the number of subjects in each sub-group are shown in Table 1. Besides participants included in the CBF analysis, non-overlapping samples with various AD endophenotypes were studied further for evaluating their associations with the CBF findings. See Fig. 1 for detailed information of participant pool selection and study design of this work.

This study was approved by institutional review boards of all participating institutions and written informed consent was obtained from all participants or authorized representatives.

2.4. MRI data acquisition and processing

Both high-resolution structural MRI data and resting ASL data were downloaded from the ADNI website (adni.loni.usc.edu). Image processing used a SPM12 (http://www.fil.ion.ucl.ac.uk/spm) based toolbox, ASLtbx (Wang *et al.*, 2008), as described previously (Wang *et al.*, 2013). ASL images were processed with the following steps: motion correction (MoCo) (Wang, 2012), temporal denoising, spatial smoothing, CBF quantification, outlier cleaning, partial volume

correction (PVC) (Hu *et al.*, 2010), spatial registration to the Montreal Neurology Institute (MNI) standard brain space, and CBF extraction in ROI.

Mean CBF for four ROIs were studied, including left angular, right angular, left temporal and right temporal gyri. The ROIs were selected on the basis FDG-PET literature (Chen *et al.*, 2011; Landau *et al.*, 2011; Wang *et al.*, 2013). In particular, meta-region-of-interest (meta-ROI) was previously found to be sensitive to AD-related CBF changes (Chen *et al.*, 2011) and originally developed for FDG-PET data (Landau *et al.*, 2011), where FDG-PET and ASL showed similar patterns of reduction in brain regions covered by these ROIs. A follow-up study also explored these ROIs using the same parcellation template and demonstrated the sensitivity of CBF on these ROIs for early AD. See Supplementary Methods for detailed MRI data acquisition, processing and analysis.

A total of 299 subjects were included in the ASL-MRI processing. To restrict the present analysis to non-Hispanic Caucasians, 258 subjects were identified based on population stratification information from genotyping data processing. Considering the relatively small number of samples for the genetic analysis, we performed further quality control to reduce the potential influence of extreme outliers. Mean and standard deviation of CBF measures for each ROI were calculated, blind to diagnostic information. Subjects who had at least one value greater or smaller than six standard deviations from the mean value of each of four CBF variables were detected as outliers. No subjects were identified as outliers and removed from this criterion. Finally, 258 subjects with four lists of quality controlled CBF measures were included (Fig. 1).

2.5. CSF Biomarkers

The total tau (t-tau) and amyloid-β 1-42 peptide ($A\beta_{1-42}$) measured in the baseline CSF samples were obtained from the ADNI database (adni.loni.usc.edu). Sample acquisition and quality control of CSF were performed as described previously (Shaw *et al.*, 2009). The t-tau/$A\beta_{1-42}$ ratio was calculated for 919 subjects who were non-Hispanic Caucasians as well as not included in the CBF analysis. Further quality control was performed to reduce the potential influence of extreme outliers on statistical results. Mean and standard deviation of t-tau/$A\beta_{1-42}$ ratio were calculated, while subjects with greater or smaller than six standard deviation from the mean value were regarded as outliers. 13 subjects were removed, where 12 subjects had missing t-tau/$A\beta_{1-42}$ measures, and 1 subject had extremely high t-tau/$A\beta_{1-42}$ ratio. Finally, 906 subjects with quality-controlled CSF t-tau/$A\beta_{1-42}$ ratio were analyzed (Fig. 1).

2.6. FDG-PET data acquisition and processing

Given the certain agreement of CBF changes and cerebral metabolic rate of glucose on some brain regions (Chen *et al.*, 2011; Musiek *et al.*, 2012), considerable variability on some other regions was also observed. With this observation, we also examined the relationship between the CBF genetic findings and glucose metabolism measurements. Preprocessed FDG-PET scans were downloaded from the ADNI website (adni.loni.usc.edu) and processed as previously described in (Risacher *et al.*, 2015). FDG-PET scans were then aligned to the corresponding MRI scans and normalized to the MNI space as $2 \times 2 \times 2$ mm^3 voxels. ROI-level glucose metabolism measurements were further extracted based on the MarsBaR AAL atlas for 735 subjects who were not included in the CBF genetic analysis. Here we focused only on the left angular region (L-AG) on which the CBF genetic association was identified. Subjects were treated as outliers and excluded if their left angular FDG-PET measures were greater or smaller than six standard deviations from the mean value. No subjects were removed under this criterion, and finally 735 subjects with quality-controlled left angular FDG-PET measured glucose metabolism were analyzed (Fig. 1).

2.7. Genotyping data

Genotyping data were obtained from the ADNI database (adni.loni.usc.edu). They were quality-controlled, imputed and combined as described in (Kim *et al.*, 2013a). Briefly, genotyping was performed on all ADNI participants following manufacturer's protocol using blood genomic DNA samples and Illumina GWAS arrays (610-Quad, OmniExpress, or HumanOmni2.5-4v1) (Saykin *et al.*, 2010). Quality control was performed in PLINK v1.90 (Purcell *et al.*, 2007) using the following criteria: 1) call rate per marker ≥ 95%, 2) minor allele frequency (MAF) ≥ 5%, 3) Hardy Weinberg Equilibrium (HWE) test $P \geq 1.0E\text{-}6$, and 4) call rate per participant ≥ 95%. Significant relatedness pairs with PI_HAT > 0.45 were identified and thereafter one individual from each pair was randomly excluded (similar to the approach applied in (Ramanan *et al.*, 2015)). Participants were then checked for gender and identity-by-descent before imputation to identify genotyping or coding error and to avoid the potential confounding effect due to the gender ambiguity or consanguinity such as sibling pairs. To restrict the studied participants to non-Hispanic Caucasians, we further performed population stratification using 988 subjects with known ancestry information from HapMap3 as reference data. We merged the ADNI and HapMap3 samples, and performed multidimensional scaling analysis using PLINK v1.90 with identity-by-state (IBS) pairwise distance matrix on the merged data to clustering samples in the principal component analysis (PCA) space. ADNI participants were identified as non-Hispanic

Caucasians if: 1) they were clustered with HapMap3 CEU or TSI subjects as well as had self-reported race/ethnicity as “non-Hispanic/white”, or 2) they were not clustered with any HapMap3 subjects while had self-reported race/ethnicity as “non-Hispanic/white”. Haplotype patterns from the 1,000 Genomes Project reference panel were then applied to impute the SNPs that were not directly genotyped from arrays. 5,574,300 SNPs were obtained for all subjects involved in this work (see Supplementary Methods for more details about genotyping data imputation). To appropriately control for population stratification, we used PLINK v1.90 to generate the top four principal components to be included as covariates in our genetic association analyses.

A list of 24 AD candidate genes from the large scale meta-analysis (Lambert *et al.*, 2013) were analyzed. Given that the Genome Reference Consortium Human build 37 (GRCh37) was used as reference genome for genotyping, gene annotation from GRCh37 was employed to extract SNPs located within each AD gene. Two genes *(HLA-DRB*1 and *HLA-DRB*5) had no SNPs available in our imputed genotyping data. In total, 4,033 SNPs were included in the genetic association analysis. Detailed information of these genes is available in Supplementary Table 1.

2.8. Statistical analysis

Targeted genetic association analysis of CBF on each ROI was tested using linear regression under an additive genetic model in PLINK v1.90 (Purcell *et al.*, 2007). Age, gender *APOE* ε4 status and the top four principal components from population stratification analysis were included as covariates. Post-hoc analysis used Bonferroni correction for adjusting both the number of SNPs and the number of quantitative traits. Regional genetic association plot was generated using LocusZoom (Pruim *et al.*, 2011). Gene-based association analysis was employed to gain comprehensive statistical evidence of genetic findings. We used GATES (Li *et al.*, 2011) to calculate a gene-level summary *P*-value for each gene by taking into account gene size, linkage disequilibrium (LD) and constituent SNP level *P*-values.

Phenotypic variance explained by an identified genetic variant was evaluated using the linear regression after removing effects from age, gender, *APOE* ε4 status and the top four principal components from population stratification analysis. Both linear regression coefficient *P* value and Cohen’s *d* statistic were used to illustrate the significance and effect size of identified variant, to facilitate the comparison among different genotyping groups.

The additive effects of the identified genetic variants from above association analysis were also assessed at each voxel using SPM12 under one-way ANOVA test with age, gender, *APOE* ε4 status and the top four principal components from population stratification analysis as

covariates. The statistical analysis results were assessed at $P < 0.001$ with no correction. The genetic effects were mapped onto the brain via voxel-based analysis.

Genetic findings from the CBF analysis were further investigated in non-overlapping samples regarding their associations with the CSF t-tau/$A\beta_{1-42}$ ratio and left angular FDG-PET glucose metabolism. For both association tests, linear regression models were used. In particular, we applied additive genetic models implemented in PLINK v1.90 (Purcell *et al.*, 2007), with age, gender, *APOE ε*4 status and the top four principal components from population stratification analysis as covariates.

3. Results

3.1. Participant characteristics

A total of 258 ADNI subjects were studied in the CBF genetic association analysis (see Table 1 for their characteristics). There were 25 subjects with missing CBF measures in one or more ROIs (2 subjects for left angular region, 2 subjects for right angular region, 12 subjects for left temporal region, and 11 subjects for right temporal region). Using one-way ANOVA or Chi-squared test, significant differences among diagnostic groups were observed for MMSE scores (P = 2.20E-16) and *APOE ε*4 status (present of *APOE ε*4 or not; P = 0.0015), while not observed for age, gender or any CBF measure.

3.2. Targeted genetic association of CBF

To identify the genetic predictor of CBF, we performed a targeted genetic association analysis (N = 258) of CBF measurements in four brain ROIs using AD risk genes and controlling for age, gender, *APOE ε*4 status and the top four principal components from population stratification analysis. A total of 4,033 SNPs located in AD candidate genes were studied.

Genetic association analysis identified one significant association between rs61068452 with L-AG CBF (P = 1.48E-7; corrected P = 2.39E-3) after correcting for the number of variants and the number of phenotypes using the Bonferroni method. The minor allele G of rs61068452 (rs61068452-G) was associated with higher CBF in L-AG compared to its major allele A (Fig. 2B). It explained an additional 9.57% of the phenotypic variance of L-AG CBF that exhibited the protective effect on AD. Significant difference of L-AG CBF existed between AA and AG groups (P = 1.43E-4), between AA and GG groups (P = 1.53E-5), and between groups AG and GG (P = 0.24). The recessive homozygote showed higher Cohen's d statistics when compared with other two groups (i.e., Cohen's d = 2.52 between AA and GG groups, Cohen's d = 1.45 between AG and GG groups and Cohen's d = 0.78 between AA and AG groups). In addition, *INPP5D*

rs61068452-G was associated with increased L-AG CBF in all diagnostic groups (Supplementary Fig. 2A).

The SNP rs61068452 resides in an intron of *INPP5D*, a reported AD candidate gene involved in inflammatory responses (Fig. 2A). Rs35349669, another SNP located within *INPP5D*, has been reported as risk AD variant in several studies (Lambert *et al.*, 2013; Ruiz *et al.*, 2014; Farfel *et al.*, 2016; Jing *et al.*, 2016). In our CBF genetic studies, no significant association of rs35349669 was observed with CBF for any region ($P > 0.05$) based on the studied samples.

Due to the possible opposite effects of our reported variant rs61068452 and previously reported variant rs35349669, we assessed their relationship. Correlation between these two SNPs was -0.22, according to the genotyping data from the studied 258 subjects. There existed no linkage disequilibrium between these two SNPs, with $r^2 = 0.046$ computed from the genotyping data of the studied 258 samples (see Supplementary Fig. 1).

We further investigated the effect of the *APOE ε*4 allele (rs429358) due to its well-known association with AD diagnosis. We did not observe significant association of rs429358 with CBF in four ROIs in the studied sample. Fig. 3 illustrated the additive effect of *INPP5D* rs61068452 on CBF under voxel-wise analysis, adjusted for age, gender, *APOE* ε4 status and the top four principal components from the population stratification analysis. The minor allele (G) of rs61068452 was associated with higher CBF, with significant clusters for this effect observed primarily in L-AG.

3.3. Gene-based association analysis of CBF

Complementary analysis was employed to test the gene-based association with CBF measures in L-AG. We assessed the gene-based association with L-AG CBF using 4,033 SNP statistics in GATES (Li *et al.*, 2011). Two genes displayed significant associations with L-AG CBF including *INPP5D* (P = 1.5E-3) and *CD2AP* (CD2 associated protein; P = 2.0E-2), after Bonferroni correction for the number of genes (Supplementary Table 2).

3.4. Association of *INPP5D* rs61068452 with CSF t-tau/Aβ1-42 ratio

Given the effect of rs61068452 with CBF measures in brain region, we hypothesized that *INPP5D* rs61068452 would also be associated with CBF related AD biomarkers. We tested the hypothesis through assessing the association of rs61068452 with CSF t-tau/$A\beta_{1-42}$ ratio in 906 subjects (Supplementary Table 3) from ADNI who were not included in the CBF genetic analysis. The minor allele (G) of rs61068452 was significantly associated with lower CSF t-

tau/$A\beta_{1\text{-}42}$ ratio (P = 0.014; Fig. 4A) under linear regression with age, gender, *APOE* ε4 status and the top four principal components as covariates. We also tested the relevance of the previously reported *INPP5D* SNP rs35349669, and identified its association with higher CSF t-tau/$A\beta_{1\text{-}42}$ ratio (P = 0.028). We observed that the minor allele (G) of rs61068452 was associated with decreased CSF t-tau/$A\beta_{1\text{-}42}$ ratio across all diagnostic groups (Supplementary Fig. 2B).

3.5. Association of *INPP5D* rs61068452 with FDG-PET

Recent studies have reported different relationships between ASL MRI and FDG-PET in different brain regions, including the similar abnormalities in some regions (Chen *et al.*, 2011; Musiek *et al.*, 2012) and decoupling between perfusion and metabolism in other brain regions (Cha *et al.*, 2013). We first explored the association of rs61068452 with glucose metabolism of left angular region measured by FDG-PET in 735 subjects from ADNI who were not included in our previous CBF analysis (Supplementary Table 4). There existed no significant association between rs61068452 and left angular glucose metabolic rate (P = 0.111, Fig. 4B) under linear regression with age, gender, *APOE* ε4 status and the top four principal components as covariates; while the minor allele (G) of rs61068452 showed a trend of association with increased glucose metabolic rate in L-AG for all diagnostic groups except healthy controls (Supplementary Fig. 2C).

3.6. Association of *INPP5D* rs61068452 with AD

To examine whether the genetic finding from our CBF analysis is directly associated with the AD status, we leveraged the valuable results available from the most recent large-scale genome-wide meta-analysis of AD (Jansen et al., 2019). According to the summary statistics of the Phase 3 analysis in this study, rs61068452 exhibited a significant association with AD (P = 1.54E-04; N = 456,488). The corresponding effect size is -0.0164, indicating a protective role of rs61068452-G in AD. This aligns well with our CSF finding.

4. Discussion

Targeted genetic analysis of AD candidate genes discovered a novel association between the SNP rs61068452 in *INPP5D* and a regional CBF measure in 258 ADNI subjects. To the best of our knowledge, this is among the first genetic association analyses of CBF measured by ASL perfusion MRI in AD-related studies. We identify that *INPP5D* rs61068452-G is associated with higher CBF of left angular gyrus. The protective effect of the G allele of rs61068452 is further

validated in a large meta-analysis of AD (*N* = 456,488), as well as shown in non-overlapping samples from ADNI, where it is associated with AD CSF biomarker (*N* = 906) and left angular glucose metabolism measured by FDG-PET (*N* = 735).

INPP5D is a known negative regulator of inflammation, and has been reported to be associated with late-onset AD in a large meta-analysis of GWAS case control study (Lambert *et al.*, 2013; Yoshino *et al.*, 2017). It has been further investigated and reviewed for its function in a number of pathways including microglial activation, neuroinflammation, and immune response (Malik *et al.*, 2015; López González *et al.*, 2016; Yoshino *et al.*, 2017). *INPP5D* mRNA analysis has revealed significantly higher expression in AD than in healthy control subjects, and suggested its involving role in microglial function via *DAP12* (DNAX-activating protein of 12kD) (Yoshino *et al.*, 2017).

INPP5D encodes a protein called *SHIP1* (phosphatidylinositol-3,4,5-trisphosphate-5-phosphatase 1). Our reported SNP rs61068452 is an intronic variant of *INPP5D*, locating nearby the *INPP5D* transcription starting site, which is related to the regulation of *SHIP1* by modulating the SH2 (Src Homology 2) domain. Therefore, one possible role which rs61068452 could play is to regulate the production of *SHIP1*. Another previously reported AD risk variant, *INPP5D* SNP rs35349669, is not associated with CBF phenotypes in the studied samples. However, it is significantly associated with CSF t-tau/$A\beta_{1\text{-}42}$ ratio in the subsequent biomarker analysis with opposite effect direction compared to rs61068452. There are multiple transcription factors of *INPP5D* for modulating the production of *SHIP1*. The SNPs rs61068452 and rs35349669 are located in different introns and independent from each other according to their linkage disequilibrium value. In addition, rs61068452 resides in regions that are related to the SH2-domain, while rs35349669 resides in regions regulating endonuclease. Thus, it warrants further investigation to examine how the molecular functions of rs61068452 and rs35349669 differ.

Recent studies of mouse model also indicate the important role of *INPP5D* in AD, especially in microglia. In particular, a recent work has demonstrated the conservative of transcriptomic between human and mouse microglia, and illustrated the higher expression level of *INPP5D* in them (Gosselin *et al.*, 2017). In another study of AD immune basis, overlap of AD associated variants within *INPP5D* with increasing enhancer has been identified in AD mouse model, as well as overlap with immune enhancer in human $CD14^{+}$ primary cells (Gjoneska *et al.*, 2015). Our reported variant, *INPP5D* rs61068452, overlaps with this enhancer region and is only ~10K bp from these variants. The transcription site nearby which rs61068452 is located encodes SH2 domain. Therefore, this may indicate a possible function of rs61068452 for modulating the transcription of *SHIP1* through affecting the SH2 domain. This provides

evidences for using mouse model to gain a better understanding of human neurodegenerative diseases.

In addition to *INPP5D*, our gene-based association analysis also discovered *CD2AP* (CD2 associated protein) associated with left angular CBF. Recent studies have identified interactions between *INPP5D* and several other AD candidates and studied their associations with AD pathogenesis. In particular, *SHIP1*, protein encoded by *INPP5D*, complexes with *CD2AP* to inhibit the ubiquitination of pro-inflammatory proteins Syk (spleen tyrosine kinase) and FcγRIIa (CD32) (Bao *et al.*, 2012). *SHIP1* has also been investigated for inhibiting *TREM2* (triggering receptor expressed on myeloid cell 2) signaling by binding to *DAP12* and preventing the recruitment of PI3K (phosphatidylinositol 3-kinase) to *DAP12* (Peng *et al.*, 2010; Malik *et al.*, 2015; Yoshino *et al.*, 2017). Functional interactions among these genes may help supply meaningful information for understanding the underlying molecular mechanism.

Pathologically, interactions between CBF and neuroinflammation and their effects on neurodegenerative diseases have been explored. CBF is regulated by activations of neurons and glial cells, including microglia which are the main resident immune cells in brain. Increased activation of microglia has been shown linked to neurodegenerative diseases including AD. Relationships between microglia and brain blood flow have also been largely studied (Attwell *et al.*, 2010; Szalay *et al.*, 2016), further suggesting their involvements in AD.

In this work, we discover that rs61068452-G is associated with higher CBF in L-AG. Given that hypoperfusion of L-AG is an established imaging biomarker of AD and early AD (Liu *et al.*, 2015; Suwa *et al.*, 2015), increased L-AG CBF in the G-carriers of rs61068452 may represent a protective role in AD neuropathogenesis. It is further validated in a large meta-analysis of AD for the protective effect of G-carriers of rs61068452.

According to the discovery of rs61068452 from targeted genetic analysis, we test its association with other AD endophenotypes including CSF t-tau/$A\beta_{1-42}$ ratio and glucose metabolism measured by FDG-PET. The minor allele (G) of rs61068452 is significantly associated with lower CSF t-tau/$A\beta_{1-42}$ ratio and shows a trend towards higher glucose metabolic rate in left angular region. Both CSF and FDG-PET hold promise as early markers for preclinical of AD, while CSF biomarkers have been thought to be a type of “AD signature”, due to their predictive power for accurate and early diagnosis of AD (Blennow *et al.*, 2015; De Deyn, 2015; Skillbäck *et al.*, 2015). Therefore, these findings further suggest the protective effect of the G allele of rs61068452 for AD.

In conclusion, we have revealed a novel association between the minor allele (G) of *INPP5D* rs61068452 and higher left angular cerebral blood flow, and have related this genetic

finding to AD endophenotypes including CSF t-tau/$A\beta_{1-42}$ ratio. This study has focused on AD candidate genes, given the modest sample size in a genetic association study. Future investigation is warranted to conduct a replication study with larger sample(s) from independent cohorts. Another future direction is to perform the longitudinal CBF analysis for characterizing disease progression. The molecular mechanism of identified *INPP5D* rs61068452 warrants further investigation, including how it modulates *SHIP1* transcription, interacts with other AD genes like *TREM2*, *CD2AP*, and affects the microglia activation and inflammation. Another future topic is to examine the biological role of *INPP5D* rs61068452 in vascular system, given the evolving of vascular system on CBF controlling and brain functions. In addition, AD animal models merit further investigation and may provide helpful information for filling the gap between neurodegenerative disease mechanisms and genetic risk and protective factors.

Acknowledgements

This work was supported in part by NIH R01 EB022574, R01 LM011360, R01 AG060054, U19 AG024904, R01 AG019771, P30 AG010133, R01 LM012535, and R03 AG054936, and by NSF IIS 1837964.

Data collection and sharing for this project was funded by the Alzheimer's Disease Neuroimaging Initiative (ADNI) (National Institutes of Health Grant U01 AG024904) and DOD ADNI (Department of Defense award number W81XWH-12-2-0012). ADNI is funded by the National Institute on Aging, the National Institute of Biomedical Imaging and Bioengineering, and through generous contributions from the following: AbbVie, Alzheimer’s Association; Alzheimer’s Drug Discovery Foundation; Araclon Biotech; BioClinica, Inc.; Biogen; Bristol-Myers Squibb Company; CereSpir, Inc.; Cogstate; Eisai Inc.; Elan Pharmaceuticals, Inc.; Eli Lilly and Company; EuroImmun; F. Hoffmann-La Roche Ltd and its affiliated company Genentech, Inc.; Fujirebio; GE Healthcare; IXICO Ltd.; Janssen Alzheimer Immunotherapy Research & Development, LLC.; Johnson & Johnson Pharmaceutical Research & Development LLC.; Lumosity; Lundbeck; Merck & Co., Inc.; Meso Scale Diagnostics, LLC.; NeuroRx Research; Neurotrack Technologies; Novartis Pharmaceuticals Corporation; Pfizer Inc.; Piramal Imaging; Servier; Takeda Pharmaceutical Company; and Transition Therapeutics. The Canadian Institutes of Health Research is providing funds to support ADNI clinical sites in Canada. Private sector contributions are facilitated by the Foundation for the National Institutes of Health (www.fnih.org). The grantee organization is the Northern California Institute for Research and Education, and the study is coordinated by the Alzheimer’s Therapeutic Research Institute at

the University of Southern California. ADNI data are disseminated by the Laboratory for Neuro Imaging at the University of Southern California.

Disclosure statement

The authors have no actual or potential conflicts of interest.

References

Attwell D, Buchan AM, Charpak S, Lauritzen M, MacVicar BA, Newman EA. Glial and neuronal control of brain blood flow. Nature 2010

Bangen KJ, Clark AL, Edmonds EC, Evangelista ND, Werhane ML, Thomas KR, et al. Cerebral blood flow and amyloid-β interact to affect memory performance in cognitively normal older adults. Front. Aging Neurosci. 2017; 9: 1–14.

Bao M, Hanabuchi S, Facchinetti V, Du Q, Bover L, Plumas J, et al. CD2AP/SHIP1 Complex Positively Regulates Plasmacytoid Dendritic Cell Receptor Signaling by Inhibiting the E3 Ubiquitin Ligase Cbl. J. Immunol. 2012; 189: 786–792.

Blennow K, Dubois B, Fagan AM, Lewczuk P, De Leon MJ, Hampel H. Clinical utility of cerebrospinal fluid biomarkers in the diagnosis of early Alzheimer's disease. Alzheimer's Dement. 2015; 11: 58–69.

Cha YHK, Jog MA, Kim YC, Chakrapani S, Kraman SM, Wang DJJ. Regional correlation between resting state FDG PET and pCASL perfusion MRI. J. Cereb. Blood Flow Metab. 2013; 33: 1909–1914.

Chen Y, Wolk DA, Reddin JS, Korczykowski M, Martinez PM, Musiek ES, et al. Voxel-level comparison of arterial spin-labeled perfusion MRI and FDG-PET in Alzheimer disease. Neurology 2011; 77: 1977–1985.

De Deyn PP. Dementia: Cerebrospinal fluid biomarkers in dementias. Nat. Rev. Neurol. 2015; 11: 549–550.

Farfel JM, Yu L, Buchman AS, Schneider JA, De Jager PL, Bennett DA. Relation of genomic variants for Alzheimer disease dementia to common neuropathologies. Neurology 2016; 87: 489–496.

Gjoneska E, Pfenning AR, Mathys H, Quon G, Kundaje A, Tsai LH, et al. Conserved epigenomic signals in mice and humans reveal immune basis of Alzheimer's disease. Nature 2015; 518: 365–369.

Gosselin D, Skola D, Coufal NG, Holtman IR, Schlachetzki JCM, Sajti E, et al. An environment-

dependent transcriptional network specifies human microglia identity. Science (80-.). 2017; 356: 1248–1259.
Hays CC, Zlatar ZZ, Wierenga CE. The Utility of Cerebral Blood Flow as a Biomarker of Preclinical Alzheimer's Disease. Cell. Mol. Neurobiol. 2016; 36: 167–179.
Hu WT, Wang Z, Lee VMY, Trojanowski JQ, Detre JA, Grossman M. Distinct cerebral perfusion patterns in FTLD and AD. Neurology 2010
Jack CR, Knopman DS, Jagust WJ, Shaw LM, Aisen PS, Weiner MW, et al. Hypothetical model of dynamic biomarkers of the Alzheimer's pathological cascade. Lancet Neurol. 2010; 9: 119–128.
Jansen IE, Savage JE, Watanabe K, Bryois J, Williams DM, Steinberg S, et al. Genome-wide meta-analysis identifies new loci and functional pathways influencing Alzheimer's disease risk. Nat. Genet. 2019
Jing H, Zhu J-X, Wang H-F, Zhang W, Zheng Z-J, Kong L-L, et al. INPP5D rs35349669 polymorphism with late-onset Alzheimer's disease: A replication study and meta-analysis. Oncotarget 2016; 7: 69225–69230.
Kim S, Swaminathan S, Inlow M, Risacher SL, Nho K, Shen L, et al. Influence of Genetic Variation on Plasma Protein Levels in Older Adults Using a Multi-Analyte Panel. PLoS One 2013a; 8: e70269.
Kim SM, Kim MJ, Rhee HY, Ryu CW, Kim EJ, Petersen ET, et al. Regional cerebral perfusion in patients with Alzheimer's disease and mild cognitive impairment: Effect of APOE Epsilon4 allele. Neuroradiology 2013b; 55: 25–34.
de la Torre J. The Vascular Hypothesis of Alzheimer's Disease: A Key to Preclinical Prediction of Dementia Using Neuroimaging. J. Alzheimers. Dis. 2018; 63: 35–52.
Lambert JC, Ibrahim-Verbaas CA, Harold D, Naj AC, Sims R, Bellenguez C, et al. Meta-analysis of 74,046 individuals identifies 11 new susceptibility loci for Alzheimer's disease. Nat. Genet. 2013; 45: 1452–1458.
Landau SM, Harvey D, Madison CM, Koeppe RA, Reiman EM, Foster NL, et al. Associations between cognitive, functional, and FDG-PET measures of decline in AD and MCI. Neurobiol. Aging 2011; 32: 1207–1218.
Li MX, Gui HS, Kwan JSH, Sham PC. GATES: A rapid and powerful gene-based association test using extended Simes procedure. Am. J. Hum. Genet. 2011; 88: 283–293.
Liu Y, Zeng X, Wang Z, Zhang N, Fan D, Yuan H. Different post label delay cerebral blood flow measurements in patients with Alzheimer's disease using 3D arterial spin labeling. Magn. Reson. Imaging 2015; 33: 1019–1025.

López González I, Garcia-Esparcia P, Llorens F, Ferrer I. Genetic and transcriptomic profiles of inflammation in neurodegenerative diseases: Alzheimer, Parkinson, Creutzfeldt-Jakob and Tauopathies. Int. J. Mol. Sci. 2016; 17: 206.
Malik M, Parikh I, Vasquez JB, Smith C, Tai L, Bu G, et al. Genetics ignite focus on microglial inflammation in Alzheimer's disease. Mol. Neurodegener. 2015; 10: 1–12.
Mattsson N, Tosun D, Insel PS, Simonson A, Jack CR, Beckett LA, et al. Association of brain amyloid-β with cerebral perfusion and structure in Alzheimer's disease and mild cognitive impairment. Brain 2014; 137: 1550–1561.
Michels L, Warnock G, Buck A, Macauda G, Leh SE, Kaelin AM, et al. Arterial spin labeling imaging reveals widespread and Aβ-independent reductions in cerebral blood flow in elderly apolipoprotein epsilon-4 carriers. J. Cereb. Blood Flow Metab. 2016; 36: 581–595.
Musiek ES, Chen Y, Korczykowski M, Saboury B, Martinez PM, Reddin JS, et al. Direct comparison of fluorodeoxyglucose positron emission tomography and arterial spin labeling magnetic resonance imaging in Alzheimer's disease. Alzheimer's Dement. 2012; 8: 51–59.
Peng Q, Malhotra S, Torchia JA, Kerr WG, Coggeshall KM, Humphrey MB. TREM2- and DAP12-dependent activation of PI3K requires DAP10 and is inhibited by SHIP1. Sci. Signal. 2010; 3: ra38.
Pruim RJ, Welch RP, Sanna S, Teslovich TM, Chines PS, Gliedt TP, et al. LocusZoom: Regional visualization of genome-wide association scan results. Bioinformatics 2011; 27: 2336–2337.
Purcell S, Neale B, Todd-Brown K, Thomas L, Ferreira MAR, Bender D, et al. PLINK: A Tool Set for Whole-Genome Association and Population-Based Linkage Analyses. Am. J. Hum. Genet. 2007; 81: 559–575.
Ramanan VK, Risacher SL, Nho K, Kim S, Shen L, McDonald BC, et al. GWAS of longitudinal amyloid accumulation on 18 F-florbetapir PET in Alzheimer's disease implicates microglial activation gene IL1RAP. Brain 2015
Risacher SL, Kim S, Nho K, Foroud T, Shen L, Petersen RC, et al. APOE effect on Alzheimer's disease biomarkers in older adults with significant memory concern. Alzheimer's Dement. 2015; 11: 1417–1429.
Ruiz A, Heilmann S, Becker T, Hernández I, Wagner H, Thelen M, et al. Follow-up of loci from the International Genomics of Alzheimer's Disease Project identifies TRIP4 as a novel susceptibility gene. Transl. Psychiatry 2014; 4: 2–5.
Saykin AJ, Shen L, Foroud TM, Potkin SG, Swaminathan S, Kim S, et al. Alzheimer's Disease Neuroimaging Initiative biomarkers as quantitative phenotypes: Genetics core aims, progress,

and plans. Alzheimer's Dement. 2010; 6: 265–273.
Saykin AJ, Shen L, Yao X, Kim S, Nho K, Risacher SL, et al. Genetic studies of quantitative MCI and AD phenotypes in ADNI: Progress, opportunities, and plans. Alzheimer's Dement. 2015; 11: 792–814.
Shaw LM, Vanderstichele H, Knapik-Czajka M, Clark CM, Aisen PS, Petersen RC, et al. Cerebrospinal fluid biomarker signature in alzheimer's disease neuroimaging initiative subjects. Ann. Neurol. 2009; 65: 403–413.
Skillbäck T, Farahmand BY, Rosén C, Mattsson N, Nägga K, Kilander L, et al. Cerebrospinal fluid tau and amyloid-β<inf>1-42</inf> in patients with dementia. Brain 2015; 138: 2716–2731.
Suwa A, Nishida K, Utsunomiya K, Nonen S, Yoshimura M, Takekita Y, et al. Neuropsychological Evaluation and Cerebral Blood Flow Effects of Apolipoprotein E4 in Alzheimer's Disease Patients after One Year of Treatment: An Exploratory Study. Dement. Geriatr. Cogn. Dis. Extra 2015; 5: 414–423.
Szalay G, Martinecz B, Lénárt N, Környei Z, Orsolits B, Judák L, et al. Microglia protect against brain injury and their selective elimination dysregulates neuronal network activity after stroke. Nat. Commun. 2016; 7: 11499.
Wang Z, Aguirre GK, Rao H, Wang J, Fernández-Seara MA, Childress AR, et al. Empirical optimization of ASL data analysis using an ASL data processing toolbox: ASLtbx. Magn. Reson. Imaging 2008; 26: 261–269.
Wang Z, Das SR, Xie SX, Arnold SE, Detre JA, Wolk DA. Arterial spin labeled MRI in prodromal Alzheimer's disease: A multi-site study. NeuroImage Clin. 2013; 2: 630–636.
Yoshino Y, Yamazaki K, Ozaki Y, Sao T, Yoshida T, Mori T, et al. INPP5D mRNA Expression and Cognitive Decline in Japanese Alzheimer's Disease Subjects. J. Alzheimer's Dis. 2017; 58: 687–694.
Zhang N, Gordon ML, Goldberg TE. Cerebral blood flow measured by arterial spin labeling MRI at resting state in normal aging and Alzheimer's disease. Neurosci. Biobehav. Rev. 2017; 72: 168–175.

Table 1. Participant characteristics in CBF genetic association analysis

Diagnosis	HC	SMC	EMCI	LMCI	AD	*P* value
Number	72	16	71	57	42	-
Gender (M/F)	35/37	7/9	45/26	27/30	21/21	0.25
Age (mean±sd)	75.03±7.42	73.56±6.87	74.01±7.46	73.88±7.66	73.67±7.74	0.83
APOE ε4 present	30.99%	37.50%	40.85%	54.39%	69.05%	**1.5E-03**
MMSE (mean±sd)	29.04±1.16	29.40±0.99	28.43±1.55	27.23±2.02	23.85±2.96	**2.2E-16**
Left angular CBF (mean±sd)	50.29±23.96	51.77±22.48	50.41±20.48	51.47±24.42	43.14±21.11	0.39
Right angular CBF (mean±sd)	52.90±22.59	46.69±16.93	49.25±20.66	57.82±27.14	50.99±25.75	0.28
Left temporal CBF (mean±sd)	44.76±19.31	46.06±15.51	44.34±24.28	43.56±21.65	37.45±21.07	0.46
Right temporal CBF (mean±sd)	46.36±23.09	34.37±17.91	40.90±18.80	44.77±23.31	37.23±19.41	0.09

CBF-cerebral blood flow, AD-Alzheimer's disease, HC-healthy control, SMC-significant memory concern, EMCI-early mild cognitive impairment, LMCI-late mild cognitive impairment. *P* values were assessed due to significant differences among diagnosis groups, and were computed using one-way ANOVA (except for gender using chi-square test).

Figure Legends

Figure 1. Flowchart of participant selection and study design.

Figure 2. Association and effect of *INPP5D* rs61068452 on left angular CBF. (A) All SNPs within *INPP5D* are plotted based on their genetic association statistics -$\log_{10}$ *P* values. NCBI build 37 genomic position and recombination rates are calculated from the 1,000 Genome Project reference data. The color scale of r^2 values is used to label SNPs based on their degree of linkage disequilibrium with rs61068452. Genes in the region are labeled with arrows denoting 5'- to -3' orientation. (B) Mean left angular CBF measures and standard errors are plotted against rs61068452 genotype groups (AA, AG, and GG). *P* value indicates the association significance of rs61068452 with left angular CBF. *P* values are calculated from linear regression with age, gender, *APOE* ε4 status and the top four principal components from population stratification analysis as covariates. Cohen's *d* indicates the effect size of minor allele G (one copy or two copies) of rs61068452 on left angular CBF, after being adjusted for age, gender, *APOE* ε4 status and the top four principal components from population stratification analysis. Presence of minor allele G of rs61068452 suggests an additive effect of increasing left angular CBF and this SNP accounts for 9.57% of the phenotypic variance.

Figure 3. Effect of *INPP5D* rs61068452 on cerebral blood flow. Selected sectional slices (top) and surface renderings (bottom) represent the voxel-wise analysis of the additive effect of rs61068452-G on CBF. The color scale indicates significance (-$\log_{10}$ *P* value) of association between rs61068452 and CBF measure (i.e., GG > AG > AA). All comparisons are displayed at a voxel-wise threshold of uncorrected $P < 0.001$ with minimum cluster size of 800 voxels (approximately responding to a cluster-wise threshold of FDR-corrected $P < 0.05$). The most significant clusters are present in the left angular gyrus.

Figure 4. Association of *INPP5D* rs61068452 on CSF t-tau/Aβ_{1-42} ratio and FDG metabolism. (A) Mean CSF t-tau/Aβ_{1-42} ratio with standard errors are plotted against the rs61068452 genotype groups (i.e., AA and AG, no GG participants in this sample). *P* value and Cohen's *d* respectively indicates the significance and effect size of the association between rs60168452 and CSF t-tau/Aβ_{1-42} ratio, with age, gender, *APOE* ε4 status and the top four principal components from population stratification analysis as covariates. Presence of minor allele (G) of rs61068452 is associated with decreasing CSF t-tau/Aβ_{1-42} ratio. (B) Mean left angular FDG-PET glucose metabolism with standard errors are plotted against the rs61068452 genotype groups (i.e., AA and AG, no GG participants in this sample). Presence of minor allele

(G) of rs61068452 is associated with increasing FDG-PET measured glucose metabolism in left angular gyrus.

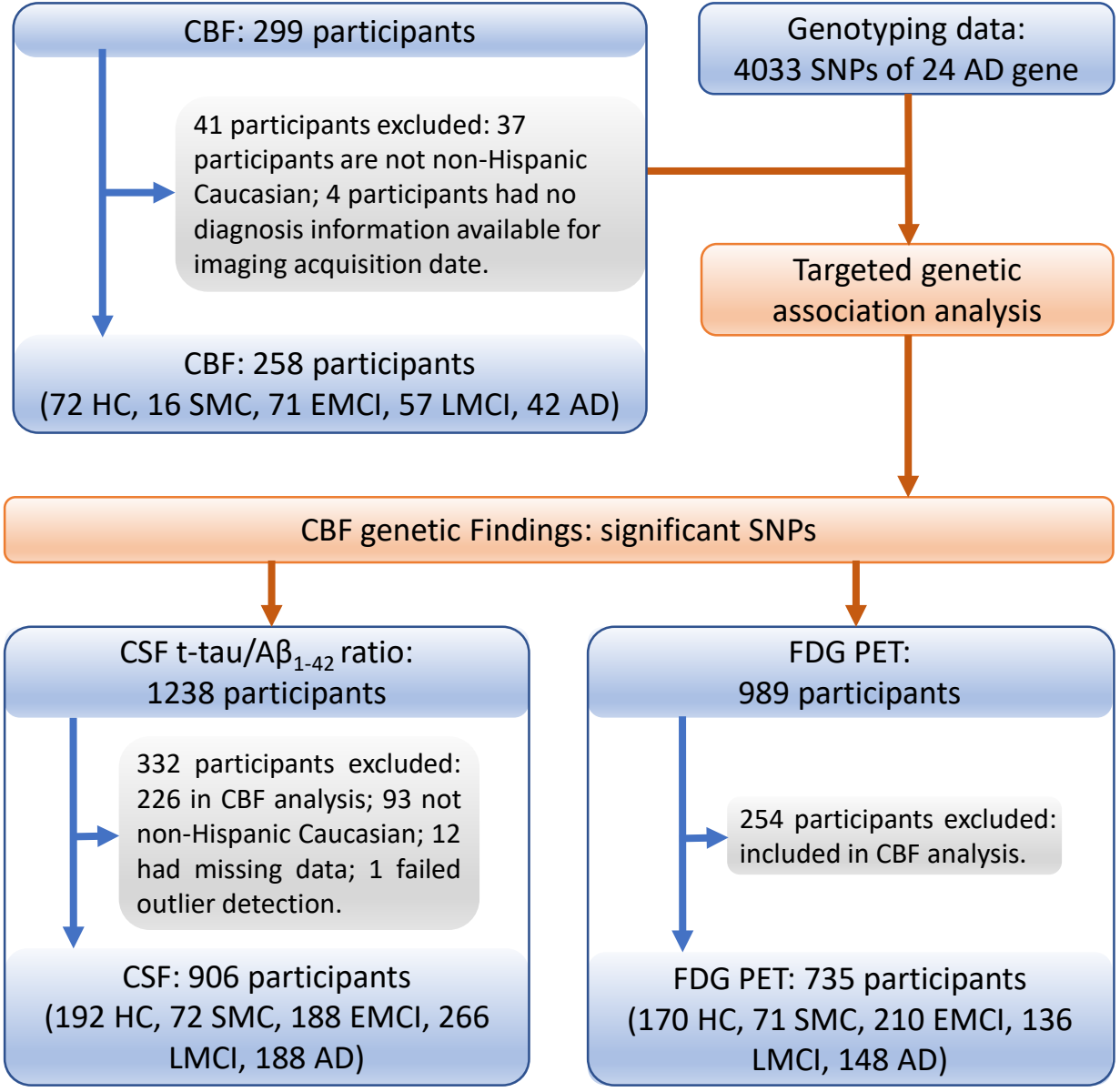
CBF: 299 participants
41 participants excluded: 37 participants are not non-Hispanic Caucasian; 4 participants had no diagnosis information available for imaging acquisition date.
CBF: 258 participants
(72 HC, 16 SMC, 71 EMCI, 57 LMCI, 42 AD)
Genotyping data:
4033 SNPs of 24 AD gene
Targeted genetic association analysis
CBF genetic Findings: significant SNPs
CSF t-tau/Aβ1-42 ratio:
1238 participants
332 participants excluded: 226 in CBF analysis; 93 not non-Hispanic Caucasian; 12 had missing data; 1 failed outlier detection.
CSF: 906 participants
(192 HC, 72 SMC, 188 EMCI, 266 LMCI, 188 AD)
FDG PET:
989 participants
254 participants excluded: included in CBF analysis.
FDG PET: 735 participants
(170 HC, 71 SMC, 210 EMCI, 136 LMCI, 148 AD)

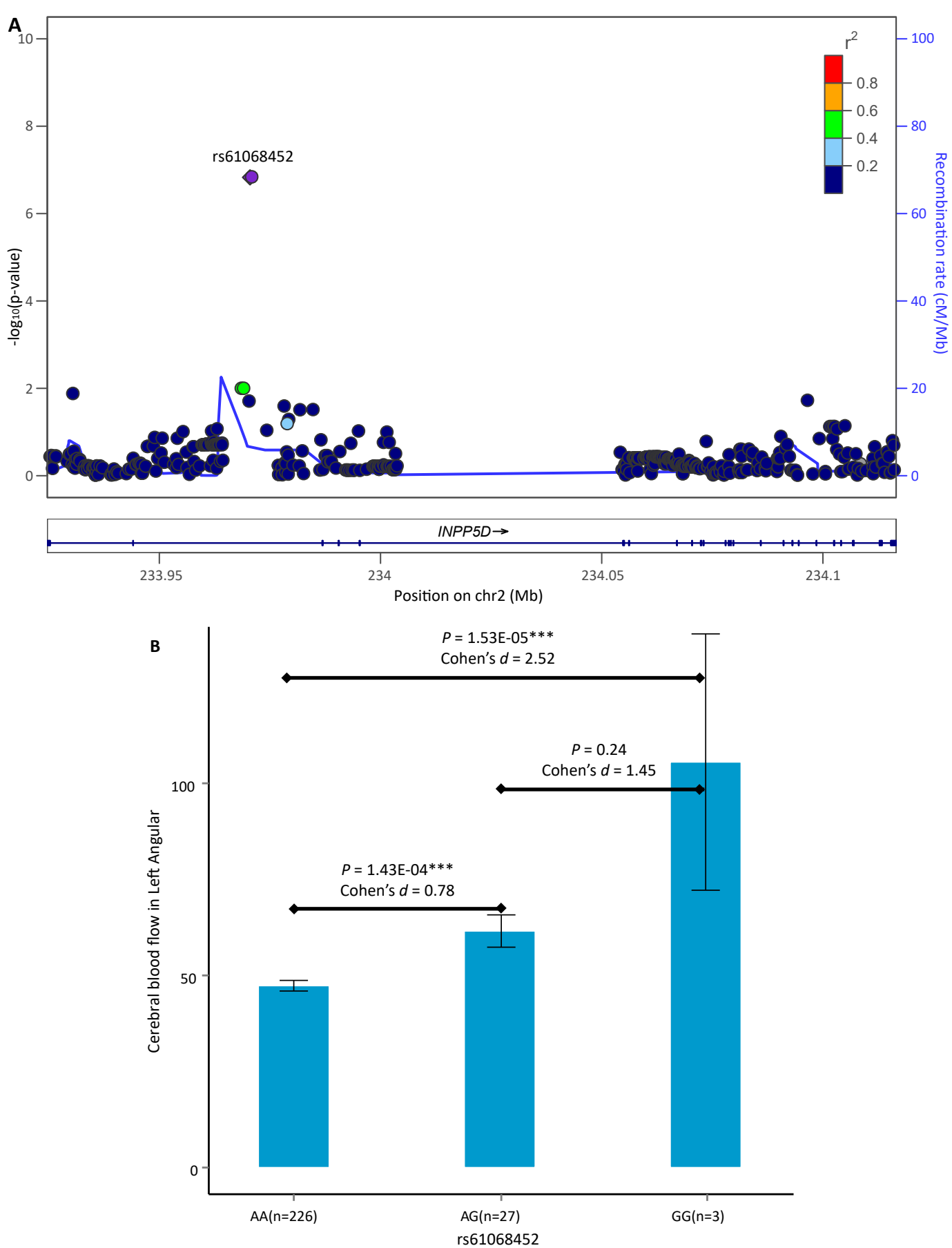
A
rs61068452
r2
0.8
0.6
0.4
0.2
-log10(p-value)
Recombination rate (cM/Mb)
INPP5D
233.95
234
234.05
234.1
Position on chr2 (Mb)
B
P = 1.53E-05***
Cohen's d = 2.52
P = 0.24
Cohen's d = 1.45
P = 1.43E-04***
Cohen's d = 0.78
Cerebral blood flow in Left Angular
AA(n=226)
AG(n=27)
GG(n=3)
rs61068452

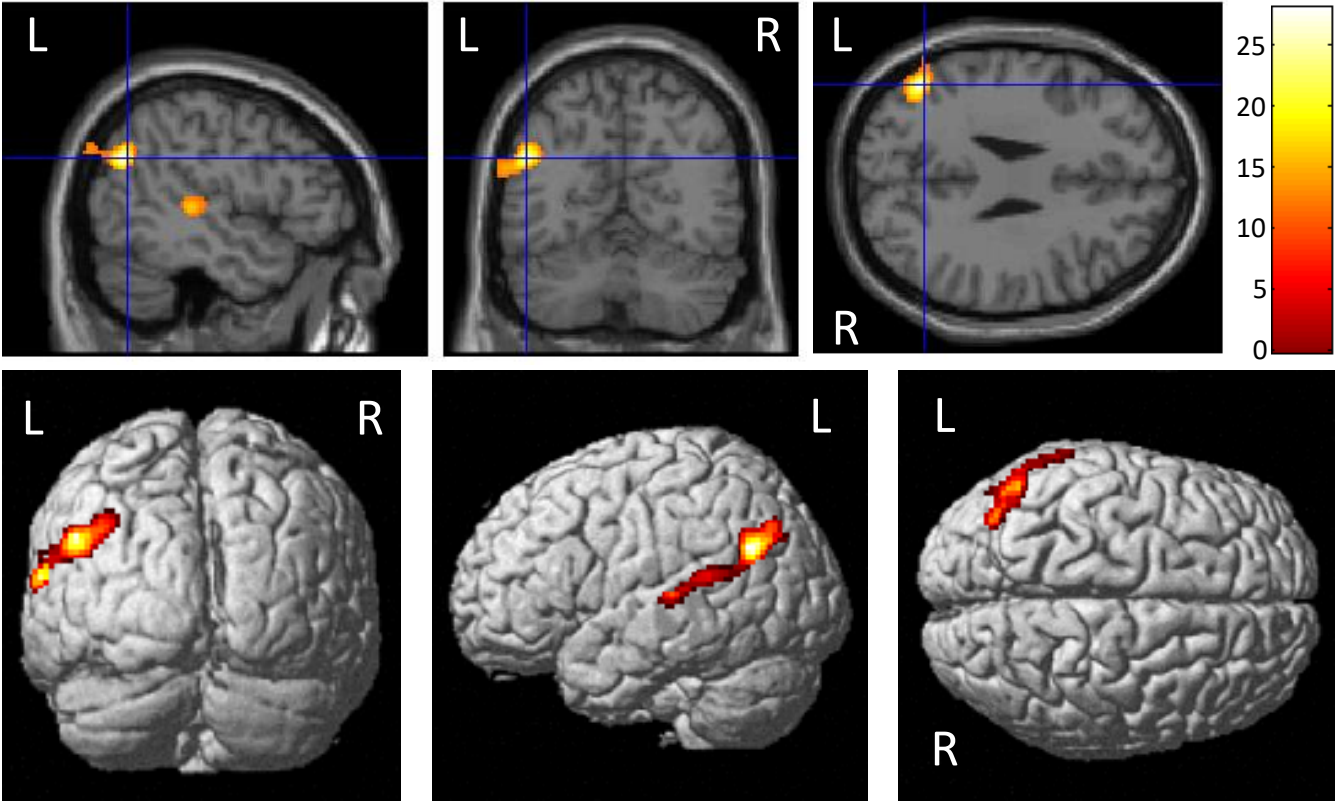
L
L
R
L
R
25
20
15
10
5
0
L
R
L
L
R

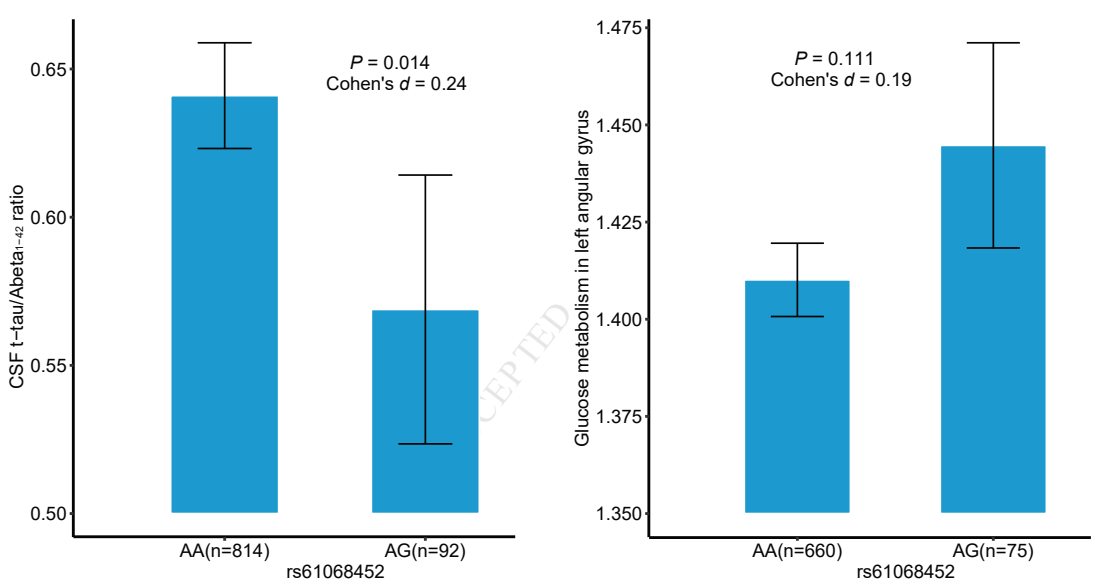
P = 0.014
Cohen's d = 0.24
CSF t−tau/Abeta1−42 ratio
0.65
0.60
0.55
0.50
AA(n=814)
AG(n=92)
rs61068452
P = 0.111
Cohen's d = 0.19
Glucose metabolism in left angular gyrus
1.475
1.450
1.425
1.400
1.375
1.350
AA(n=660)
AG(n=75)
rs61068452